

Novel Ferrocenyl Polyene Derivatives and Their Binding to Unmodified Cyclodextrins

Jian Liu,[†] René Castro,[†] Khalil A. Abboud,[‡] and Angel E. Kaifer^{*†}

Center for Supramolecular Science and Department of Chemistry, University of Miami, Coral Gables, Florida 33124-0431, and Chemistry Department, University of Florida, Gainesville, Florida 32611

akaifer@miami.edu

Received April 17, 2000

Two new ferrocene derivatives, 7-ferrocenyl-2,4,6-heptatrienal (**1**) and 7-ferrocenyl-2,4,6-heptatrienol (**2**), were synthesized and characterized. These two compounds possess a rigid triene chain conjugated to one of the cyclopentadienyl rings of the ferrocene residue, and as a result, they exhibit very stiff structures. The electronic absorption and electrochemical properties of these compounds were utilized to investigate their host–guest binding interactions with the receptors α -cyclodextrin (α -CD) and β -cyclodextrin (β -CD) in aqueous solution. From electronic absorption measurements binding constants in the range 790–12900 M⁻¹ were obtained; β -CD formed more stable complexes than α -CD with both guests. Electrochemical measurements suggest some degree of site selectivity in the complexation processes, with β -CD binding preferentially to the ferrocene moiety while α -CD interacts with the unsaturated chain.

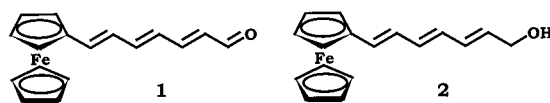
Introduction

Ferrocene and its derivatives are well-known guests for complexation by the three unmodified cyclodextrins (CDs).¹ While β -CD forms the most stable complex with the ferrocene moiety, α -CD and γ -CD also exhibit reasonable binding affinity. This binding selectivity has been exploited by our group in the past. For instance, we have reported the binding interactions between cationic ferrocenyl derivatives containing aliphatic chains of variable length and α - and β -CD hosts.² Electrochemical and NMR spectroscopic data demonstrated that β -CD binds preferentially to the ferrocene residue while α -CD interacts selectively with the aliphatic chain. These findings provided the basis for the preparation of α -CD-based zwitterionic rotaxanes³ and, more recently, α -CD rotaxanes supported on gold nanospheres.⁴

Several significant reasons led us to extending these investigations to systems in which the aliphatic chain is replaced by a conjugated polyene chain. First, conjugation throughout the molecule may increase the level of electronic communication between the two possible binding sites (the ferrocenyl residue and the polyene chain). Second, the ferrocenyl polyene guests are extremely rigid guests with well-defined molecular regions. Third, threading of a conjugated polyene chain through the cavity of

a CD host may give rise to an inclusion complex that presents interesting analogies to a neuronal axon, with the insulating CD host surrounding the electronically conducting, conjugated nucleus. Therefore, we decided to prepare two novel ferrocenyl polyene derivatives (compounds **1** and **2**, see structures below) and investigate their binding properties to α - and β -CD.

STRUCTURES



Results and Discussion

Synthesis. The synthetic route to compounds **1** and **2** is summarized in Scheme 1. First, the commercially available 1-(trimethylsilyloxy)-1,3-butadiene (**3**) was treated with triethylorthoformate with zinc chloride as the catalyst to yield 5,5'-diethoxypenta-2-enal (**4**) in 84% yield.⁵ Under Wittig conditions, this compound gave 6,6'-diethoxy-1-bromo-1,3-pentadiene⁶ (74%), which, after lithiation with *t*-BuLi, was treated with ferrocenecarboxaldehyde to produce (after treatment with HBr during the workup)⁷ the deep red 7-ferrocenyl-2,4,6-heptatrienal (**1**) in 40% yield after recrystallization from dichloromethane/hexane. 7-Ferrocenyl-2,4,6-heptatrienol (compound **2**) was obtained as a red solid (78% yield) by reduction of **1** with LAH.⁸ Compounds **1** and **2** were fully characterized by NMR spectroscopy, MS, and elemental analysis.

(5) Akgun, E.; Pindur, U. *Synthesis* **1984**, 227.

(6) Duhamel, L.; Duhamel, P.; Lecouve, J.-P. *Tetrahedron* **1987**, *43*, 4349.

(7) Duhamel, L.; Ple, G.; Ramondec, Y. *Tetrahedron Lett.* **1989**, *30*, 7377.

(8) Smith, M. B. *Organic Synthesis*; McGraw-Hill: New York, 1994; Chapter 4.

* To whom correspondence should be addressed. Tel: (305) 284-3468. Fax: (305) 444-1777.

[†] University of Miami.

[‡] University of Florida.

(1) (a) Harada, A.; Takahashi, S. *J. Chem. Soc., Chem. Commun.* **1984**, 645. (b) Matsue, T.; Evans, D. H.; Osa, T.; Kobayashi, N. *J. Am. Chem. Soc.* **1985**, *107*, 3411. (c) Menger, F. M.; Sherrod, M. J. *J. Am. Chem. Soc.* **1988**, *110*, 8606. (d) Thiem, H.-J.; Brandl, M.; Breslow, R. *J. Am. Chem. Soc.* **1988**, *110*, 8612. (e) Stoddart, J. F.; Zarzycki, R. *Recl. Trav. Chim. Pays-Bas* **1988**, *107*, 515. (f) Kaifer, A. E. *Acc. Chem. Res.* **1999**, *32*, 62.

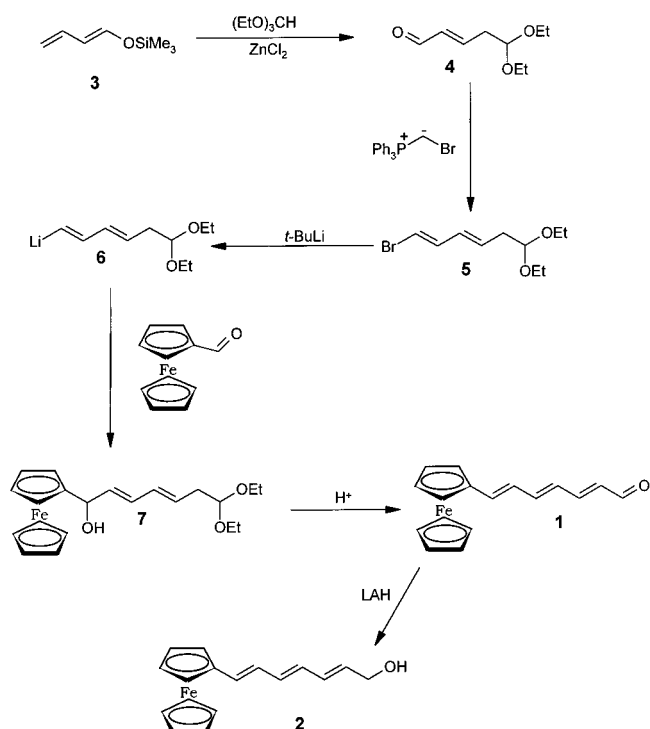
(2) Isnin, R.; Salam, C.; Kaifer, A. E. *J. Org. Chem.* **1991**, *56*, 35.

(3) (a) Isnin, R.; Kaifer, A. E. *J. Am. Chem. Soc.* **1991**, *113*, 8188.

(b) Isnin, R.; Kaifer, A. E. *Pure Appl. Chem.* **1993**, *65*, 495.

(4) Liu, J.; Xu, R.; Kaifer, A. E. *Langmuir* **1998**, *14*, 7337.

Scheme 1



X-ray Crystal Structure of 1. Single crystals of **1** were obtained from dichloromethane/hexane solution. The corresponding X-ray crystal structure [space group P2(1)] is shown in the Supporting Information. As anticipated, this structure exhibits a rigid sidearm that is fully conjugated and, thus, coplanar with the adjacent cyclopentadienyl ring of the ferrocene subunit. The crystal packing of the molecules is best described by a series of rows in which the rigid chain of each ferrocene derivative extends so that the terminal aldehyde oxygen reaches close to the next ferrocene nucleus. All the ferrocene groups in each of these rows maintain a well-defined alignment with their main axes parallel to one another. The angle of the ferrocene groups changes, alternating between two main orientations, from row to row.

Electrochemical and Visible Spectroscopic Studies. As anticipated, the electrochemical behavior of compounds **1** and **2** is dominated by the one-electron oxidations of their ferrocene subunits.⁹ To assess the effects that the conjugated unsaturated chains exert on the electrochemical parameters, we also investigated ferrocenecarboxaldehyde (**8**) and ferrocenemethanol (**9**). These model compounds have the same terminal groups as **1** and **2**, respectively, but lack the connecting unsaturated tether. The relevant voltammetric parameters are given in Table 1. Notice that all compounds exhibit fast heterogeneous electron-transfer behavior in cyclic voltammetric experiments as revealed by the peak-to-peak potential splitting values (ΔE_p) in Table 1. Therefore, the voltammetric behavior of compounds **1** and **2** is reversible in acetonitrile solution, as is usually the case for the one-electron oxidation of most ferrocene derivatives.⁹ The corresponding half-wave potentials reveal that the unsaturated tether tends to facilitate the oxidation process. For instance, the $E_{1/2}$ value for **1** is less positive than that

Table 1. Voltammetric and Spectroscopic Parameters for Ferrocene Derivatives **1**, **2**, **8**, and **9** in Acetonitrile Solution at 25 °C

compd	$E_{1/2}^a$ (V vs SSCE)	ΔE_p^b (mV)	λ_{\max} (nm)	ϵ ($M^{-1}\cdot\text{cm}^{-1}$)
1	0.46	59	560	4730
2	0.40	59	500	1600
8	0.69	58	458	500
9	0.42	59	438	100

^a Half-wave potentials obtained from square wave voltammetry measurements in $\text{CH}_3\text{CN}/0.1 \text{ M TBAPF}_6$. ^b Potential difference between the anodic and cathodic peak potentials observed in cyclic voltammetry experiments at a scan rate of 0.1 V/s.

for **8**. The same trend is observed with **2** and **9**, as the first compound shows a slightly lower $E_{1/2}$ value. These potential values indicate that the unsaturated chain injects electronic density into the ferrocene moiety, acting as an electron donor substituent.

It is also interesting to compare the difference between the $E_{1/2}$ values for the oxidation of compounds **1** and **2** with the difference between the values for **8** and **9**. As anticipated from the electron withdrawing character of the aldehyde group and the electron donor character of the CH_2OH group, the aldehyde shows a higher oxidation potential in both pairs of compounds. However, while the $\Delta E_{1/2}$ value is rather large for the latter pair ($\sim 0.27 \text{ V}$ more positive for the aldehyde), the corresponding difference is much smaller for compounds **1** and **2** (0.06 V more positive for the aldehyde). This finding indicates that the unsaturated tether attenuates the electronic differences exerted by the terminal functional groups on the electroactive ferrocene subunit, thus revealing that the electronic communication along the triene chain is not very effective. Other groups have reported poor transmission of electronic effects through unsaturated chains¹⁰ similar to those present in compounds **1** and **2**.

The visible spectra of compounds **1** and **2** reveal the extended conjugation afforded by the unsaturated tethers. As evidenced by the data in Table 1, the λ_{\max} values shift to the red and the molar absorptivities increase with the number of conjugated bonds present in the ferrocene derivatives.

Complexation Studies. Due to the hydrophobic character of the ferrocene subunit and the triene chain, compounds **1** and **2** exhibit extremely low solubilities in aqueous media. However, the solubility of either compound is substantially enhanced by the presence of α -CD or β -CD in the aqueous solution. Figure 1 shows the electronic absorption spectra of aqueous solutions saturated with **2** and containing variable concentrations of α -CD. Clearly, the solubility of **2** increases with the concentration of α -CD in the medium. This CD-induced solubility enhancement of the ferrocene derivative can be explained by the formation of a stable complex between **2** and α -CD. These spectroscopic data can be used to determine the equilibrium constant for the

(9) Kaifer, A. E.; Gómez-Kaifer, M. *Supramolecular Electrochemistry*; Wiley-VCH: Weinheim, 1999; Chapter 2.

(10) (a) Creager, S.; Yu, C. J.; Bamdad, C.; O'Connor, S.; MacLean, T.; Lam, E.; Chong, Y.; Olsen, G. T.; Luo, J.; Gozin, M.; Kayyem, J. F. *J. Am. Chem. Soc.* **1999**, *121*, 1059. (b) Davis, W. B.; Svec, W. A.; Ratner, M. A.; Wasielewski, M. R. *Nature* **1998**, *396*, 60. (c) Sachs, S. B.; Dudek, S. P.; Hsung, R. P.; Sita, L. R.; Smalley, J. F.; Newton, M. D.; Feldberg, S. W.; Chidsey, C. E. D. *J. Am. Chem. Soc.* **1997**, *119*, 10563. (d) Tolbert, L. M.; Zhao, X.; Ding, Y.; Bottomley, L. A. *J. Am. Chem. Soc.* **1995**, *117*, 12891. (e) Benniston, A.; Gouille, V.; Harriman, A.; Lehn, J.-M.; Marczinke, B. *J. Phys. Chem.* **1994**, *98*, 7798. For reviews, see: (f) Kohler, B. E. *Chem. Rev.* **1993**, *93*, 41. (g) Orlandi, G.; Zerbetto, F.; Zgierski, M. Z. *Chem. Rev.* **1991**, *91*, 867. (h) Allen, M. T.; Whitten, D. G. *Chem. Rev.* **1989**, *89*, 1691. (i) Tolbert, L. M. *Acc. Chem. Res.* **1992**, *25*, 561.

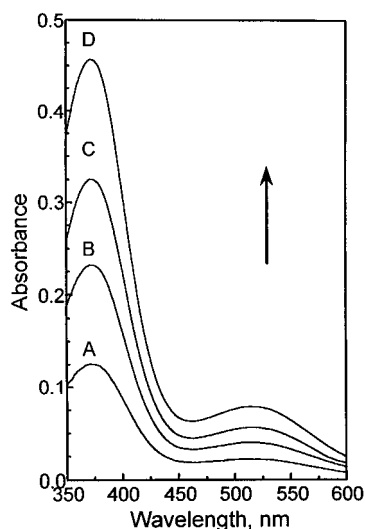


Figure 1. Electronic absorption spectra of aqueous solutions (0.2 M NaCl) saturated in **2** and also containing (A) 5 mM α -CD, (B) 10 mM α -CD, (C) 15 mM α -CD, and (D) 20 mM α -CD. Optical path length: 1.0 cm.

Table 2. Binding Constants (M^{-1}) for the Association of Ferrocene Derivatives **1 and **2** with α - and β -CD Hosts in 0.05 M NaCl at 25 °C**

guest	host	
	α -CD	β -CD
1	790 ± 20	$12\,200 \pm 270$
2	2300 ± 130	$12\,900 \pm 150$

association of the ferrocene derivative with the CD host (see Experimental Section). The binding constant values obtained are given in Table 2. The values are generally higher than those obtained with cationic ferrocene derivatives with pendant aliphatic chains.² This finding may perhaps result from the structural rigidity and marked hydrophobic character of the ferrocene triene guests surveyed in this work. Both guests exhibit a higher binding constant with β -CD than with α -CD. The chain's terminal group of the guest ($-\text{CH}_2\text{OH}$ vs $-\text{CHO}$) does not change significantly the binding constant with β -CD, but it does influence the binding constant with α -CD. This finding may reflect the different binding sites presented by **1** and **2** for each CD host. Unfortunately, the structural characterization of the complexes was hampered by the low aqueous solubility of the guests, which made impossible a detailed NMR investigation of their interactions with CD hosts. Our attempts to crystallize the complexes have been fruitless so far.

If β - and α -CD interact with compounds **1** and **2** at different molecular sites it should be possible to form ternary complexes with either guest. This possibility was addressed by investigating the solubility enhancement induced by mixtures of α - and β -CD. The corresponding experimental data are given in Figure 2. Figure 2 shows the maximum absorbances (measured at 500 nm) for saturated solutions of **2** containing variable concentrations of CD hosts. The key finding is that a mixture of 5 mM α -CD and 5 mM β -CD dissolves more **2** than would be expected from the sum of the individual effects of either host. This cooperative effect is most logically explained by the presence in solution of a ternary complex formed by one molecule of β -CD, one molecule of α -CD, and one guest molecule.

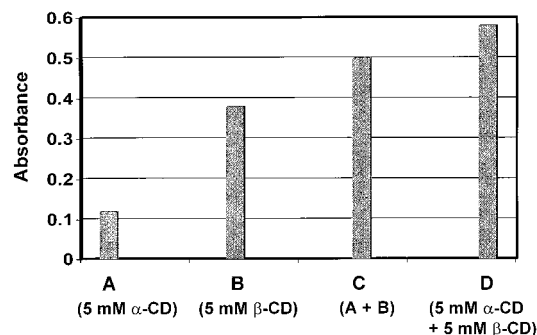


Figure 2. Absorbances measured at 500 nm of saturated solutions of **2** containing 0.2 M NaCl and variable concentrations of CD hosts.

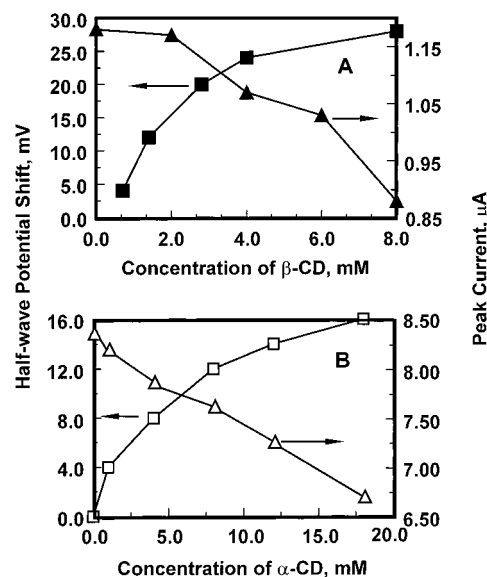


Figure 3. CD-induced effects on the voltammetric parameters of guest **2**. (A) β -CD effects (0 to 8 mM) on the half-wave potential (\blacksquare) and the peak current (\blacktriangle) recorded with a solution containing 0.05 mM **2** + 20 mM α -CD + 0.2 M NaCl. (B) α -CD effects (0 to 20 mM) on the half-wave potential (\square) and the peak current (\triangle) recorded with a solution containing 0.235 mM **2** + 6 mM β -CD + 0.2 M NaCl.

Despite the low solubility of **1** and **2** in aqueous media, voltammetric techniques were also used to investigate these complexes. In one series of experiments, the solubility of compound **2** was enhanced by the presence of 20 mM α -CD in the solution. The reversible oxidation of the ferrocene moiety in **2** was then monitored as a function of the concentration of β -CD added to this solution. The results are summarized in Figure 3A. Clearly, the half-wave potential for the oxidation of **2** shifts to more positive values and the anodic peak currents decrease as the concentration of the β -CD host increases. These two lines of electrochemical evidence are consistent with the formation of an inclusion complex between the ferrocene subunit of the guest and β -CD.^{1b,2} This conclusion is further supported by the β -CD-induced increase in the ΔE_p values observed in cyclic voltammetric experiments under these conditions. The availability of the ferrocene moiety for complexation by β -CD in the presence of a large excess of α -CD suggests again that the latter host binds the guest at a different site.

Similar experiments were carried out but this time **2** was solubilized by the presence of 6 mM β -CD. The

voltammetric behavior of **2** was then monitored as increasing concentrations of α -CD were added to this solution. The results are shown in Figure 3B. Notice that much higher concentrations of α -CD are needed to observe smaller changes in the half-wave potential as compared to the results recorded in the reverse experiments (Figure 3A). The clear indication from these voltammetric experiments is that the main binding site for α -CD is the unsaturated chain, while the preferred binding site for β -CD is the ferrocene moiety.

In conclusion, we have reported the synthesis of two new ferrocene derivatives with a rigid unsaturated triene chain that is conjugated to the cyclopentadienyl ring to which is covalently attached. The formation of host-guest complexes between these new ferrocene compounds and the hosts α - and β -CD was demonstrated using electrochemical and spectrophotometric measurements, although the detailed structural characterization of these complexes was restricted by the low aqueous solubility of the guests. In any instance, the structural stiffness of these ferrocenyl derivatives and the reactivity of their terminal functional groups (aldehyde and hydroxyl) suggests that these compounds may find applications in the synthesis of more complicated supramolecular systems.

Experimental Section

Materials. All chemicals were of the best quality commercially available and were used as obtained unless otherwise noted. All reactions were performed under nitrogen in dried glassware. THF and acetonitrile were freshly distilled. Column chromatography was performed with Scientific Adsorbents silica gel (63–200 μ m). Water for the electrochemical and binding studies was purified with a 4-cartridge Barnstead Nanopure purification system.

5,5'-Diethoxypenta-2-enal (4). ZnCl₂ in Et₂O solution (35.1 mL of 1 M solution, 35.1 mmol) was added slowly to a solution of 1-(trimethylsilyloxy)-1,3-butadiene (10 g, 70.3 mmol) and triethylorthoformate (12.5 g, 84.3 mmol) in CH₂Cl₂ (100 mL) at room temperature. The clear solution was stirred for 1 h. NaHCO₃ (satd, 100 mL) was added and the mixture stirred until gas evolution ceased. Additional NaHCO₃ (20 mL) was added until the mixture was slightly basic. The organic phase was separated and dried over Na₂SO₄, and the solvent was removed under vacuum. The product was isolated as a yellow oil (10.2 g, 84% yield): ¹H NMR (400 MHz, CDCl₃) δ 1.20 (6H, t), 3.30–3.80 (4H, m), 4.62 (1H, t), 5.40–6.80 (2H, m), 9.45 (1H, d).

5,5'-Diethoxy-1-bromo-1,3-pentadiene (5). Potassium *tert*-butoxide (57.6 mL of 1 M solution in THF, 57.6 mmol) was added over 10 min to a suspension of bromomethyltriphenyl phosphonium bromide (25 g, 57.3 mmol) in THF (300 mL) at –70 °C. After 1.5 h, 5,5-diethoxypenta-2-enal (7.9 g, 45.8 mmol) in THF (20 mL) was added slowly over 10 min. Then the reaction mixture was allowed to warm to 0 °C, and the mixture stirred for 1 h. After this, the reaction mixture was allowed to warm to room temperature and stirred for another 1.5 h. H₂O (80 mL) was added, the solution was stirred for 10 min and concentrated, and the aqueous layer was extracted with Et₂O. The organic fractions were dried over Na₂SO₄ and concentrated under vacuum. Column chromatography (CH₂Cl₂/(CH₃)₂CO, 9:1) on silica gel was used to isolate the product as a brown oil (8.4 g, 74% yield): ¹H NMR (400 MHz, CDCl₃) δ 1.20 (6H, t), 2.50 (1H, s), 3.50–3.70 (4H, m), 4.50 (1H, t), 5.70–6.60 (4H, m).

7-Ferrocenyl-2,4,6-heptatrienal (Compound 1). *t*-BuLi (40.5 mL of a 1.5 M solution in pentane, 60.7 mmol) was added to a stirred solution of the bromoacetal (8.4 g, 33.9 mmol) in anhydrous Et₂O (160 mL) at –70 °C. After 80 min, ferrocene-carboxaldehyde (5.8 g, 27.1 mmol) in Et₂O (40 mL) was added. The temperature was raised to 0 °C and the reaction mixture

stirred for 1.5 h. NaHCO₃ (5% aq, 80 mL) was added, the aqueous phase was extracted with Et₂O, and the combined organic phases were washed with H₂O until the washings were neutral, dried over Na₂SO₄, and concentrated under vacuum. The product was hydrolyzed by refluxing in a mixture of acetone (216 mL), H₂O (1.2 mL), and HBr (47%, 6 drops). After 1 h, the solution was neutralized with NaHCO₃ (5% aq, 20 mL), concentrated, and partitioned between H₂O and CHCl₃. The aqueous phase was washed with chloroform, the organic extracts were dried over Na₂SO₄, and the solvent evaporated under vacuum. Recrystallization of the product from hexane: dichloromethane (9:1) solution yields **1** as a red crystalline solid (3.16 g, 40%): ¹H NMR (400 MHz, CDCl₃) δ 4.12 (5H, s), 4.18 (2H, t), 4.22 (2H, t), 6.15–6.78 (6H, m), 9.58 (1H, d); FAB MS (3-nitrobenzyl alcohol) *m/z* 292 (M⁺). Anal. Calcd for C₁₇H₁₆OFe: C, 69.89; H, 5.52. Found: C, 69.92; H, 5.59.

7-Ferrocenyl-2,4,6-heptatrienol (Compound 2). Lithium aluminum hydride (LAH, 28.4 mg, 0.75 mmol) in 20 mL of THF was added to a solution of **1** (292 mg, 1 mmol) in 20 mL of THF at –78 °C. The solution was stirred under N₂ for 1.5 h. Additional LAH (28.4 mg, 0.75 mmol) was added. The reaction was monitored by TLC and quenched with Rochelle's salt solution (potassium sodium tartrate tetrahydrate, 20% aq., 20 mL) after the disappearance of the TLC spot corresponding to compound **1**. The reaction mixture was filtered, concentrated, and partitioned between H₂O and CH₂Cl₂ (50 mL each). The aqueous layer was washed with CH₂Cl₂. The combined organic phase was washed with H₂O (2 \times 20 mL), dried over Na₂SO₄, and concentrated. Column chromatography (CH₂Cl₂/ethyl acetate, 3:1) on silica gel gave pure **2** as an orange red solid (225 mg, 78% yield): ¹H NMR (400 MHz, CDCl₃) δ 4.12 (5H, s), 4.20 (2H, s), 4.28 (2H, t), 4.38 (2H, t), 5.82–6.44 (6H, m); FAB MS (3-nitrobenzyl alcohol) *m/z* 294 (M⁺). Anal. Calcd for C₁₇H₁₈OFe: C, 69.41; H, 6.17. Found: C, 69.02; H, 5.93.

X-ray Experimental Data. Data were collected at 173 K on a Siemens SMART PLATFORM equipped with a CCD area detector and a graphite monochromator utilizing Mo K α radiation ($\lambda = 0.71073$ Å). Cell parameters were refined using up to 8192 reflections. A hemisphere of data (1381 frames) was collected using the ω -scan method (0.3° frame width). The first 50 frames were remeasured at the end of data collection to monitor instrument and crystal stability (maximum correction on *I* was <1%). Empirical absorption corrections were applied based on the entire data set.¹¹

The structure was solved by the Direct Methods in SHELX-TL5¹² and refined using full-matrix least squares. The non-H atoms were treated anisotropically, whereas the hydrogen atoms were calculated in idealized positions and were riding on their respective carbon atoms. A total of 172 parameters were refined in the final cycle of refinement using 2839 reflections with $I > 2\sigma(I)$ to yield *R*₁ and w*R*₂ of 2.50% and 6.41%, respectively. Refinement was done using *F*².

Equipment and Procedures. In the NMR spectra all chemical shifts are reported in ppm and referenced to the solvent peak present or to TMS. Molar absorptivity coefficients were determined from plots of absorbance vs concentration for sets of standard solutions. A single-compartment electrochemical cell was used for the voltammetric experiments. The working electrode was a polished glassy carbon electrode (5 mm diameter), a platinum flag served as the auxiliary electrode and a homemade sodium chloride saturated calomel electrode (SSCE) was used as the reference electrode. Before the electrochemical experiments, all solutions were deoxygenated by purging with N₂ and kept under an inert atmosphere during the experiments.

Determination of Binding Constants. The binding equilibria of guests **1** and **2** with α - and β -CD were investigated using spectrophotometric measurements. Both guests exhibit strong absorption bands around 500 nm that were particularly useful for this purpose. Since the molar absorptivity at this wavelength of guests **1** and **2** was not affected by the presence

(11) Blessing, R. H. *Acta Crystallogr.* **1995**, *A51*, 33.

(12) Sheldrick, G. M. SHELXTL5; Bruker AXS, Madison, WI, 1998.

of either CD host, the total absorbance at 500 nm is given by the sum of the absorbances due to the free guest and the complexed guests:

$$A = (\epsilon b[\text{complex}]) + (\epsilon b[\text{free guest}]) \quad (1)$$

In the absence of CD

$$A_0 = \epsilon b[\text{free guest}] \quad (2)$$

Therefore,

$$r = (A - A_0)/A_0 = [\text{complex}]/[\text{free guest}] \quad (3)$$

which leads to

$$[\text{CD}]_T = (K^{-1} + [\text{free guest}])r \quad (4)$$

where $[\text{CD}]_T$ is the analytical CD concentration and K is the binding constant for the 1:1 association equilibrium between

the guest and the CD host. According to eq 1, a plot of $[\text{CD}]_T$ vs r must be a straight line with a slope equal to $(K^{-1} + [\text{free guest}])$, from which the K value can be easily obtained since the concentration of free guest remains constant and equal to its solubility value.

Acknowledgment. The authors are grateful to the National Science Foundation for the support of this work (to A.E.K., CHE-9633434 and CHE-9982014). K.A.A. wishes to acknowledge the National Science Foundation and the University of Florida for funding the purchase of the X-ray equipment.

Supporting Information Available: Tables of crystal data and structure refinement for **1**, atomic coordinates, bond lengths and angles, and anisotropic displacement parameters. Two figures containing ORTEP and packing drawings for the crystal structure of compound **1**. This material is available free of charge via the Internet at <http://pubs.acs.org>.

JO000573U